

Friction Studies of Polymer Lubricated Surfaces<sup>†</sup>P. M. McGuiggan,<sup>\*,‡</sup> M. L. Gee,<sup>§</sup> H. Yoshizawa,<sup>||</sup> S. J. Hirz,<sup>||</sup> and J. N. Israelachvili<sup>||</sup>

National Institute of Standards and Technology, Polymers Division, Gaithersburg, Maryland 20899, School of Chemistry, University of Melbourne, Parkville, Victoria, Australia 3010, and Department of Chemical Engineering and Materials Department, University of California, Santa Barbara, California 93105

Received August 2, 2006; Revised Manuscript Received January 2, 2007

**ABSTRACT:** The shear properties of thin films of polymer melts confined between two molecularly smooth solid surfaces have been measured using a surface forces apparatus (SFA). Poly(dimethylsiloxane) (PDMS), polybutadiene (PBD), and perfluoropolyether (PFPE) of various molecular masses were studied, including both entangled and nonentangled systems. In all cases, the systems exhibited “smooth” sliding, with no intermittent or stick–slip motion at moderate shear rates (50–500 s<sup>−1</sup>). The coefficients of friction ranged from approximately 0.5 to 0.006, generally decreasing with increasing molecular mass and bulk viscosity for each polymer. The measured friction coefficients were smaller than values measured previously for lower molecular mass molecules such as *n*-alkanes, which is consistent with the above trend. During sliding, the surfaces remain separated by a thin tenacious polymer film, even at high loads where the minimum surface separation was found to be proportional to the radius of gyration,  $R_g$ , for each polymer. The friction coefficients for systems that are not entangled in the bulk are higher than for entangled systems. Shear for entangled systems appears to occur at the wall rather than within the polymer film, resulting in very low friction forces. For each type of polymer studied, one finds a decreasing friction or “effective” viscosity of the confined fluids with increasing (i) molecular mass, (ii) bulk viscosity, and (iii) degree of entanglement. These opposite trends (compared to those of the bulk fluids, including simple hydrocarbon liquids) are due to the effects of the atomically (or molecularly) structured walls on the molecular configurations of the confined fluids, and the increased film thicknesses with increasing molecular mass.

## Introduction

Most moving parts require some amount of lubrication to reduce friction and prevent wear.<sup>1</sup> The lubricant film is often a polymeric material that operates by keeping the moving parts separated, lowering the shear strength, and dissipating the heat. The performance of a material or fluid as a lubricant depends upon its dynamic properties and interaction forces with the shearing surfaces.<sup>2–4</sup> The bulk properties of lubricants have been investigated extensively in an effort to understand friction and wear.<sup>5,6</sup> However, in applications such as microelectromechanical systems (MEMS) and hard disk drives, the lubricant operates in nanometer thick films, i.e., only a few lubricant molecules thick, whose static and dynamic properties are quite different from the bulk properties.<sup>7,8</sup> Knowledge regarding the dynamic properties of thin films is crucial both for understanding the basic mechanisms of friction and lubrication, and for the development of new devices.

Previous studies of nanometer thick films under steady-state sliding focused on simple molecules.<sup>8–10</sup> The friction was measured between mica surfaces separated by simple hydrocarbon liquids of different chemical structure such as cyclohexane, tetradecane, and branched hydrocarbons such as

squalane.<sup>11–13</sup> The behavior of these fluids in thin films was found to be entirely different from the respective bulk behavior, including, for example, their measured “effective” viscosity which was generally non-Newtonian and often orders of magnitude larger than in the bulk even when compared to the elevated viscosities of the bulk fluids under similar hydrostatic pressures. The latter observations suggest that the details of the confinement, for example, the topography of the confining (and shearing) surfaces, the contact area, and the surface separation, determine the friction forces (or coefficients) rather than the load or pressure.

Recently, the shear properties of polymers under steady state and oscillatory sliding conditions have also been measured using the SFA.<sup>14–21</sup> The present work extends these studies to a variety of neat polymer melt chemistries and molecular masses both above and below the entanglement molecular mass,  $M_e$ . In particular, measurements of the steady-state sliding properties of thin films of polybutadiene and poly(dimethylsiloxane) melts are reported and the results are compared to the friction of perfluoropolyether melts, other liquids, and shorter chain molecules. Our choice of these 3 polymer melt families was based to their different chemistries (hydrocarbons, siloxanes and perfluoroethers), and general interest (hydrocarbon oils, silicone oils, and fluorocarbon polymers now commonly used in the lubrication of hard disk drives). The range of molecular masses used (from 1000 to 11 000 g/mol) also span the entanglement molecular masses.

The polymer melts are colorless, relatively inert liquids at room temperature. Previous viscosity measurements at film thicknesses  $D$  greater than the radius of gyration  $R_g$  indicate that these polymers retain their bulk viscosities except in a thin semi-immobilized layer at each wall of “hydrodynamic thickness”  $1–2 R_g$ .<sup>19,22–24</sup> The immobilized layers overlap when  $D$

<sup>†</sup> Certain commercial equipment, instruments, or materials are identified in this paper in order to adequately specify the experimental procedure. Such identification does not imply recommendation or endorsement by the National Institute of Standards and Technology nor does it imply that the materials or equipment identified are necessarily the best available for the purpose.

<sup>\*</sup> Corresponding author.

<sup>‡</sup> National Institute of Standards and Technology, Polymers Division.

<sup>§</sup> School of Chemistry, Melbourne University.

<sup>||</sup> Department of Chemical Engineering and Materials Department, University of California, Santa Barbara.

is less than 2–4  $R_g$ , taking the system into the tribological or lubrication regime of behavior. Our aim in this study was to further probe the shear properties of these “immobilized” polymer films.

## Materials and Methods

A surface forces apparatus (SFA) with a lateral sliding attachment was used to measure the shear forces.<sup>25</sup> The SFA is a powerful tool for measuring shear forces since parameters such as area of contact and surface separation can be simultaneously measured via observation of the interferometric fringes. The lateral sliding attachment shears two flattened molecularly smooth mica surfaces past each other while simultaneously controlling and/or measuring the surface separation  $D$ , sliding speed  $v$ , normal load  $L$ , molecular contact area  $A$ , pressure  $P = L/A$  and lateral shear force  $F$  or shear stress  $S = F/A$ . Typical values in this study were  $D = 1$ –8 nm,  $v = 0.5$ –1  $\mu\text{m/s}$ ,  $L = 0$ –200 mN,  $A = 10^{-6}$ – $10^{-3}$  cm<sup>2</sup>,  $F = 0$ –100 mN, and  $P = F/A = 0$ –15 MPa (i.e., 0–150 atm). Surface separations were measured to  $\pm 0.1$  nm;  $v$ ,  $L$ , and  $A$  were measured to  $\pm 5\%$ , and  $F$  was measured to  $\pm 30\%$  for the smaller friction forces (and to better accuracy for the larger friction forces). The large uncertainty in the friction force measurements is due to the extremely low values of the friction forces attained for some of these polymer melt systems. The  $\pm$  refers to the standard uncertainty in the measurements and is taken as one standard deviation of the measured values.

The mica sheets were glued to silica support cylinders using *sym*-diphenylcarbide glue. The experiments were carried out with a macroscopic droplet of liquid between the two crossed cylindrical surfaces. Solid P<sub>2</sub>O<sub>5</sub> was placed inside the apparatus to eliminate moisture (water is known to adsorb at the hydrophilic mica–polymer interface and affect the boundary slip conditions). The experimental temperature was maintained at 25 °C. The values of the molecular mass  $M_w$ , radius of gyration  $R_g$ , and bulk viscosity  $\eta$  for the polymer melts used are given in Table 1. The number following each polymer abbreviation is the molecular mass.

Polybutadiene (PBD) has the structural formula  $(-\text{CH}_2-\text{CH}=\text{CH}-\text{CH}_2-)_m$ . The samples were supplied by Lew Fetters.<sup>26</sup> Two PBD molecular masses were studied: 1000 (PBD 1000) and 3500 g/mol (PBD 3500). The PBD molecules had cis and trans bonds alternating randomly throughout the molecule with about 8% branching. The molecular chain diameter of PBD is  $\sigma = 0.45$  nm and the persistence length is  $l_p = 0.48$  nm.<sup>27,28</sup>

Poly(dimethylsiloxane) (PDMS) is a linear polymer with the structural formula  $[-\text{Si}(\text{CH}_3)_2-\text{O}-]_m$ . The molecular mass was 3700 g/mol (PDMS 3700) and was obtained from Dow Corning (Dow Corning 200, Midland, MI). The sample was relatively polydisperse with  $M_w/M_n = 2.3$ . The diameter of a PDMS chain is about 0.8 nm and the persistence length is 0.65 nm.<sup>27,28</sup>

The perfluoropolyether (PFPE) samples were obtained from Montedison, USA, Inc. and are known as Fomblin Z fluids. PFPE is a random block copolymer with the structural formula  $\text{CF}_3[(\text{OCF}_2\text{CF}_2)_p(\text{OCF}_2-\text{CF}_2)_q](\text{OCF}_2)_r\text{OCF}_3$ . Three molecular masses were studied: 4300 (PFPE 4300), 10 300 (PFPE 10 300), and 21 700 g/mol (PFPE 21 700). The diameter of a PFPE chain is 0.6–0.7 nm, and the persistence length is  $\sim 1$  nm.<sup>29–32</sup>

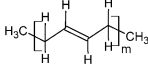
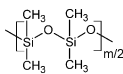
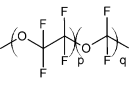
The densities of PBD, PDMS, and PFPE are 0.89, 0.96, and 1.81 g/mL, respectively. PDMS and PFPE have very flexible chains, whereas PBD has a more rigid backbone. The entanglement molecular masses  $M_e$  of PBD, PDMS, and PFPE are 1850, 9600, and 9500 g/mol, respectively.<sup>28,33</sup>

All the samples were centrifuged at 500 rad/s for 1 h immediately prior to use. Unless otherwise noted, the PDMS and PBD results were obtained at a sliding velocity of  $v = 0.5$   $\mu\text{m/s}$  whereas the PFPE measurements were taken at  $v = 1$   $\mu\text{m/s}$ .

## Results

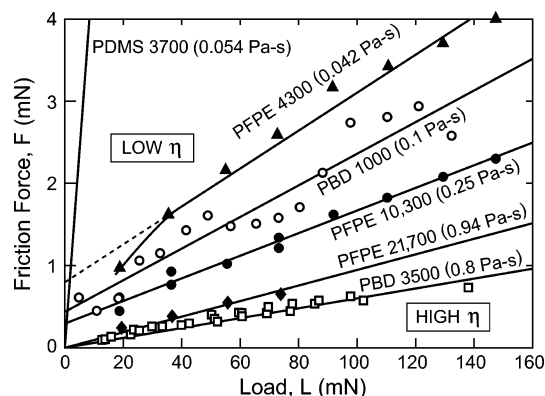
At least two complete experiments were run for each sample, and within each experiment, at least two different contact

Table 1. Polymer Melt Data and Minimum Film Thickness<sup>a</sup>

Polymer Melt		Minimum Film Thickness D (nm) ± 0.1 nm	
Bulk, molecular and intrinsic properties	Specific Properties	Without shear*	With shear (D <sub>H</sub> )
<b>PBD</b>  (-CH <sub>2</sub> -CH=CH-CH <sub>2</sub> -) <sub>m</sub>    ρ = 0.89 g/ml σ = 0.45 nm M <sub>e</sub> = 1850 g/mol l <sub>p</sub> = 0.48 nm <sup>27</sup>	PBD 1000 M <sub>w</sub> = 1000 g/mol m = 20 M <sub>w</sub> /M <sub>n</sub> = 1.08 η <sub>bulk</sub> = 0.1 Pa-s R <sub>g</sub> = 1.15 nm	3.0	3.0
	PBD 3500 M <sub>w</sub> = 3500 g/mol m = 65 M <sub>w</sub> /M <sub>n</sub> = 1.16 η <sub>bulk</sub> = 0.8 Pa-s R <sub>g</sub> = 2.2 nm	3.7	6.5
	PBD 7000 M <sub>n</sub> = 7000 g/mol m = 130 M <sub>w</sub> /M <sub>n</sub> = 1.03 η <sub>bulk</sub> = 5 Pa-s R <sub>g</sub> = 3.0 nm	10	12
<b>PDMS</b>  (-Si(CH <sub>3</sub> ) <sub>2</sub> -O-) <sub>m</sub>    ρ = 0.96 g/ml σ = 0.8 nm M <sub>e</sub> = 9600 g/mol l <sub>p</sub> = 0.65 nm <sup>27</sup>	PDMS 3700 M <sub>w</sub> = 3700 g/mol m = 50 M <sub>w</sub> /M <sub>n</sub> = 2.3 η <sub>bulk</sub> = 0.054 Pa-s R <sub>g</sub> = 1.6 nm		1.5
<b>PFPE</b>  CF <sub>3</sub> -[(OCF <sub>2</sub> CF <sub>2</sub> ) <sub>p</sub> - (OCF <sub>2</sub> ) <sub>q</sub> ]-OCF <sub>3</sub>    ρ = 1.81 g/ml σ = 0.6-0.7 nm <sup>21</sup> M <sub>e</sub> = 9500 g/mol l <sub>p</sub> = 1 nm <sup>32</sup>	PFPE 4300 M <sub>w</sub> = 4300 g/mol M <sub>w</sub> /M <sub>n</sub> = 1.3 η <sub>bulk</sub> = 0.042 Pa-s R <sub>g</sub> = 1.6 nm	5.0	2.0
	PFPE 10,300 M <sub>w</sub> = 10,300 g/mol M <sub>w</sub> /M <sub>n</sub> = 1.9 η <sub>bulk</sub> = 0.25 Pa-s R <sub>g</sub> = 3.0 nm	6.5	2.7
	PFPE 21,700 M <sub>w</sub> = 21,700 g/mol M <sub>w</sub> /M <sub>n</sub> = 1.5 η <sub>bulk</sub> = 0.94 Pa-s R <sub>g</sub> = 4.0 nm		4.0

<sup>a</sup> The asterisk denotes that minimum  $D$  without shear is the measured closest approach of two flattened mica surfaces separated by the polymer melt at loads in excess of 100 mN.

positions of the surfaces were used to measure the friction forces, surface separations (film thicknesses), contact areas, etc., as a



**Figure 1.** Measured friction forces  $F$  between mica surfaces as a function of normal load  $L$ . The surfaces are separated by thin films of various polymer melts as indicated. The solid lines are least-squares fit to the data. The slopes of the lines give the friction coefficients  $\mu$ . Sliding velocities  $v$  were in the range  $(0.5 - 1.0) \mu\text{m/s}$ . Typical error in  $F$ :  $\pm 30\%$ . The data for PDMS 3700 are out of range and are given in Figure 2.

function of load and sliding velocity. The friction forces for all the polymer melts were measured in the “tribological” regime (i.e., under high compression and confinement) where the mica surfaces were pressed into a flattened contact under a large load  $L$ , corresponding to  $P = 2\text{--}15 \text{ MPa}$ . Under these pressures, the films were thinner than  $4R_g$ . Sliding was commenced at a constant driving velocity,  $v$ , in one direction for a given distance of approximately  $100 \mu\text{m}$  or more (typically larger than the contact diameter), and then the sliding direction was reversed. In this way, sliding was continued at fixed velocities of  $\pm v$  per “cycle” until steady-state tribological conditions were reached. Once steady-state conditions were attained, usually within 1–2 cycles, the load was increased and the cycling was repeated. None of the systems exhibited stick–slip friction or stiction spikes; the friction traces were therefore fairly featureless and similar to those previously shown in ref 19, Figure 14, and ref 59, Figure 3a.

The measured friction forces  $F$  vs load  $L$  for the six polymer melts studied are shown in Figure 1. In all cases  $F$  is found to be roughly proportional to  $L$ , i.e., obeying Amontons’ law:

$$F = \mu L \quad (1a)$$

which can also be expressed in terms of the shear stress ( $S = F/A$ ) and pressure ( $P = L/A$ ):

$$S = \mu P \quad (1b)$$

When the data do not extrapolate to the origin, it is customary to define the friction coefficient  $\mu$  in terms of the slope:  $\mu = \partial F / \partial L$ . This is the definition used here since many of the “lines” in Figure 1 do not extrapolate to  $F = 0$  at  $L = 0$ . We also note that the friction coefficients of PBD 1000, PBD3500, and PDMS 3700 were relatively insensitive to the sliding velocity for speeds between  $0.5$  and  $3 \mu\text{m/s}$ , consistent with Coulomb’s law regarding the “constancy” of  $\mu$ .

The coefficients of friction,  $\mu = \partial F / \partial L$ , for PBD 1000 and PBD 3500 were found to be  $0.020 \pm 0.003$  and  $0.006 \pm 0.002$ , respectively. In comparison, under similar sliding conditions, the coefficients of friction for mica surfaces separated by thin films of octane, tetradecane, and 2-methyloctadecane have been measured to be very much higher:  $1.5$ ,  $0.8$  and  $0.39$ , respectively.<sup>34</sup> Thus, for all five of these hydrocarbon fluids, the coefficient of friction decreases as the molecular mass increases. Earlier macroscopic measurements<sup>1</sup> and recent numerical simu-

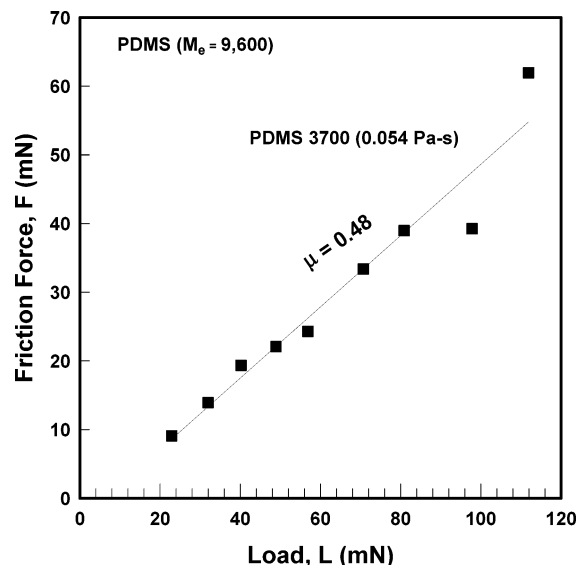


**Figure 2.** Measured friction forces  $F$  between mica surfaces as a function of normal load  $L$ . The surfaces are separated by a thin film of PDMS 3700 (■). The solid line is a least-squares fit to the data. The slope of the line is the friction coefficient  $\mu$ . The friction forces are measured to  $\pm 10\%$ .

lations<sup>35</sup> of short chain molecules also found that the coefficient of friction decreases with increasing chain length.

Figure 1 also shows the coefficients of friction measured for thin films of PFPE 4300 ( $\mu = 0.023 \pm 0.002$ ), PFPE 10 300 ( $\mu = 0.014 \pm 0.002$ ), and PFPE 21 700 ( $\mu = 0.006 \pm 0.002$ ).<sup>20</sup> Once again, for the specific polymer type (PFPE in this case), the friction force varies linearly with the load and decreases with increasing molecular mass and increasing (bulk) viscosity,  $\eta$ . Static force profiles for these polymer melts have been previously reported.<sup>23,24,36,37</sup>

The measured friction  $F$  vs load  $L$  for PDMS 3700 is shown in Figure 2. The coefficient of friction is  $0.48 \pm 0.05$ . This is approximately 2 orders of magnitude higher than the coefficient of friction for the similar molecular mass but higher bulk viscosity hydrocarbon PBD 3500.

All the polymer melts studied exhibit monotonically repulsive (normal) forces with no or little adhesion, as has been previously reported.<sup>19,23,24,36,37</sup> And, for such systems, one does expect  $F$  to be proportional to  $L$ , as was seen in these measurements.<sup>4</sup> In addition, the polymer melts studied exhibited smooth sliding. No stick–slip motion was observed. Stick–slip motion has been observed for smaller molecules such as cyclohexane, octane, and octamethylcyclotetrasiloxane confined between mica surfaces.<sup>9,25,34</sup> Stick–slip motion is expected for films having a negative slope in the  $F$  vs  $v$  curves, or for ordered, “solid-like” films whose order is broken down with increasing sliding velocity leading to a “fluid-like” film (where the abrupt reduction in the friction can be considered as a steep negative slope in the  $F(v)$  curve).<sup>38</sup> Thus, there appears to be a correlation between stick–slip, the nature of the normal forces across the film (whether attractive, repulsive, or oscillatory), and the ability of liquids to order between the surfaces. One measure of the degree of ordering is molecular in-plane layering. This is seen as discrete steps in the surface separation as the load increases, resulting in oscillatory force–distance curves. For simple molecules such as cyclohexane and octane, there is distinct in-plane layering where the distance of each step corresponds to the diameter of the intervening molecules.<sup>9,25,34</sup> Molecular-dynamics simulations of thin films of short, symmetrically shaped molecules confined between two solid stationary plates

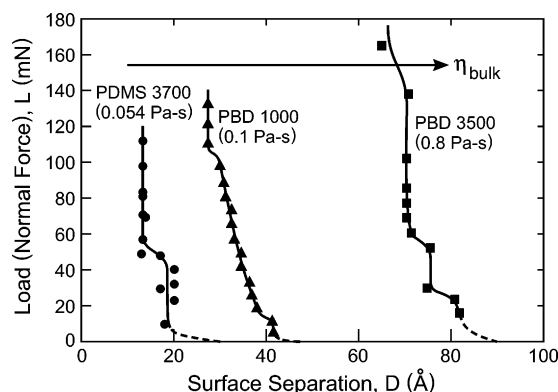


**Figure 3.** Dynamic surface separation  $D$  as a function of applied load  $L$ . The measurements were taken while the surfaces were sliding at a velocity of  $v = 0.5 \mu\text{m/s}$ . The surfaces were separated by PDMS (●), PBD 1000 (▲), and PBD 3500 (■). The solid lines are meant to guide the eye. The surface separation was measured to  $\pm 0.1 \text{ nm}$ .

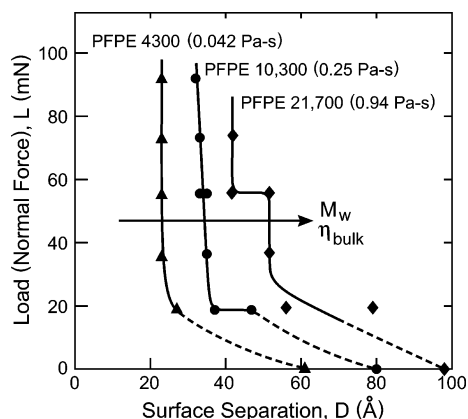


**Figure 4.** Dynamic surface separation  $D$  as a function of applied load  $L$ . The measurements were taken while the surfaces were sliding with a velocity of  $v = 1 \mu\text{m/s}$ . The surfaces were separated by PFPE 4300 (●), PFPE 10 300 (▲), and PFPE 21 700 (◆). The solid lines are meant to guide the eye. The surface separation was measured to  $\pm 0.1 \text{ nm}$ . We may note that while steps in the quasi-static normal force curves are not expected for flexible, high molecular mass polymer melts, for sheared systems under a load (as we have here and in Figure 3), shear-ordering can occur, giving rise to steps, as previously seen with squalane.<sup>11,12</sup>

have shown how ordering in such films arises:<sup>39–41</sup> as one plate is sheared past another, stick–slip motion occurs which may be due to a negative slope of the  $F$  vs  $v$  curve or to periodic freezing–melting phase transitions of the lubricant film.<sup>38,42</sup> Branched hydrocarbons, such as 2-methyloctadecane and squalane ( $\text{C}_{30}\text{H}_{62}$ ), span between layers, which makes them effectively more disordered than symmetrically shaped molecules and gives rise to the monotonically repulsive forces that have been experimentally observed.<sup>34,43</sup> Consequently, 2-methyloctadecane and squalane show little or no layering, and limited or chaotic stick–slip sliding.<sup>11,34</sup> The extent of both in-plane and out-of-plane ordering (and stick–slip) decreases as molecules become more complex.

Figures 3 and 4 show the variation in the average surface separation (film thickness)  $D$  with load, measured as the surfaces were sheared, for the six polymer melts listed in Table 1. Generally, once the initially curved surfaces flattened elastically (Hertz-like) under the influence of the externally applied compressive load, the thickness was uniform across the entire contact area at each load, as seen by the flat interference fringes. However, a rippled or nonuniform interference fringe pattern was sometimes observed during sliding, especially as the load was changed or at higher loads. Thus, the surface separation

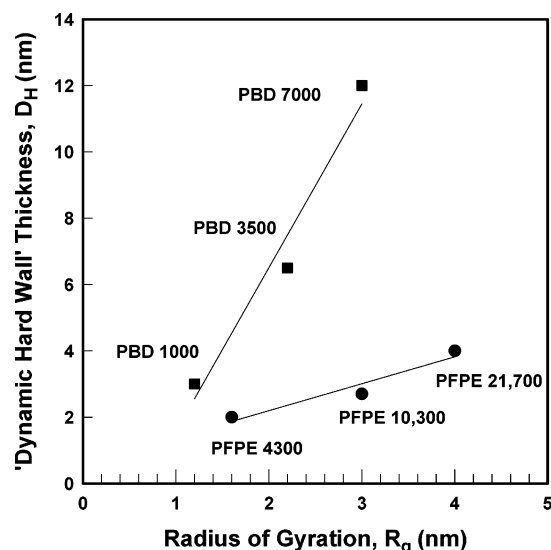


**Figure 5.** “Dynamic hard wall” surface separation (measured at loads of 100 mN) as a function of the radius of gyration of the polymer melt. The surfaces are separated by thin films of PBD (■) and PFPE (●). The solid line is a least-squares fit to the points with the slopes calculated as 3.8 and 0.81 for PBD and PFPE, respectively. There appears to be no direct correlation between the dynamic hard wall thicknesses  $D_H$  and the persistence lengths,  $l_p$ , or chain diameters,  $\sigma$  (Table 1). Clearly, some additional properties are involved in determining the hard wall thicknesses and their quantitative relationship to  $R_g$ .

sometimes varied slightly, by up to one molecular diameter, across the contact diameter. As shown in Figures 3 and 4, stepped variations in the surface separation were sometimes observed, but these were less distinct than for shorter molecules previously studied.<sup>25,34</sup> The layering effect was more pronounced for the thinner PDMS and PFPE films than for the PBD films. This implies that the PDMS and PFPE films are more ordered under shear than the thicker PBD films.

We can define a “dynamic hard wall” of thickness  $D_H$  as the minimum surface separation or film thickness measured during sliding at the highest attainable load (loads over 100 mN corresponding to pressures of 8–15 MPa) that did not damage the mica surfaces. As shown in Figure 3, the surface separation for PDMS 3700 varied from  $\sim 3.3 \text{ nm}$  at the lowest loads to  $1.5 \pm 0.1 \text{ nm}$  at the highest loads ( $P = 8 \text{ MPa}$ ). Thus,  $D_H = 1.5 \text{ nm}$ , which is one  $R_g$  of the polymer. The limiting surface separations for all the polymer melts are given in Table 1.

As shown in Figure 5,  $D_H$  appears to vary linearly with  $R_g$  and hence is inversely proportional to  $M_w$  for both PBD and PFPE. The graph also includes data for PBD 7000, where  $D_H = 12 \text{ nm}$  which was measured in an independent study.<sup>19</sup> The linear fits to the data in Figure 5 give  $D_H = 4.9R_g$  for PBD and  $D_H = 0.81R_g$  for PFPE. For PDMS, which was studied at only one molecular mass,  $D_H$  was about  $1R_g$ . Hence, for both PDMS and PFPE, the minimum surface separation achieved upon sliding corresponded to about  $1R_g$ , whereas for PBD it was about  $5R_g$ . It is interesting to note that PBD has a substantially higher film strength or load bearing capacity under shear even though it has a lower friction. As detailed in the discussion, the combination of a high degree of entanglement and the stiff backbone makes PBD a better boundary lubricant.

Finally, we compare  $D_H$  to the minimum hard wall separation measured in the absence of shear (static loading).<sup>23</sup> The results are also summarized in Table 1. For PFPE and PDMS, the surface separation decreased during shearing compared to static loading conditions. For PBD 1000, shear did not seem to affect the minimum surface separation, while for PBD 3500 and PBD



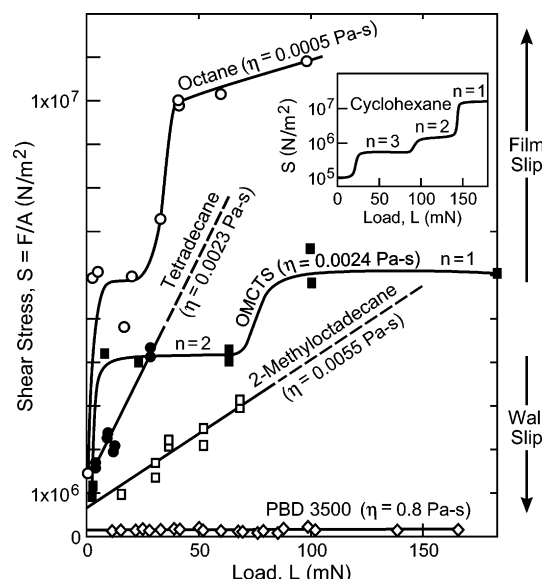


**Figure 6.** Shear stresses measured between mica surfaces separated by thin liquid films of cyclohexane, octane, tetradecane, octamethylcyclotetrasiloxane (OMCTS), 2-methyloctadecane, and PBD 3500. The solid lines are meant to guide the eye.

7000, the films thickened with shear.<sup>12,19</sup> We may note that PBD 3500 and PBD 7000 are entangled in the bulk and have a stiff polymer backbone, whereas PBD 1000, PDMS 3700 and PFPE 4300 have  $M_w < M_e$  and are more flexible than PBD. The PDMS and PFPE samples were also more polydisperse (cf. Table 1). These results suggest that entanglements and dilatancy play an important role in determining the nature and magnitude of the friction forces.

## Discussion

A summary of the measured shear stress,  $S = F/A$ , vs load  $L$  for mica surfaces separated by various liquid films, including some previously measured liquids, is given in Figure 6. For simple liquids such as cyclohexane and octane, in-plane molecular layering is observed in the thin film as seen by the stepped changes of the shear stress on load. For simple liquids, the entropic energy of confinement (including excluded volume effects) gives rise to an oscillatory short-range force, and the surfaces slide when separated by discrete layers of molecules. The shear stress is found to be quantized for each molecular layer and increases as the number of layers between the layers decreases.<sup>25,34</sup>

As the molecules become larger and more complex (asymmetric), the oscillations diminish and the entropic force becomes monotonically repulsive.<sup>24,37,44–46</sup> The friction force decreases in magnitude, and stick–slip motion is replaced by smooth sliding. The surface separation is generally larger than in the (quantized) oscillatory regime, and the friction force now increases monotonically (and often linearly) with increasing load. Figure 6 illustrates these effects, showing the dramatic dependence of the shear stress on the molecular mass and bulk viscosity: as the molecular mass and viscosity of the hydrocarbon molecules increase, the shear stress decreases.

Figure 7 shows a plot of the friction force vs the number of molecular polymer layers separating the surfaces for the six polymer melts studied. The number of molecular layers was calculated by dividing the optically measured surface separation  $D$  by the chain diameter of the specific polymer,  $\sigma$  (as given in the first column of Table 1). As seen in Figure 7, the friction increases as the number of molecular layers decreases, and rises

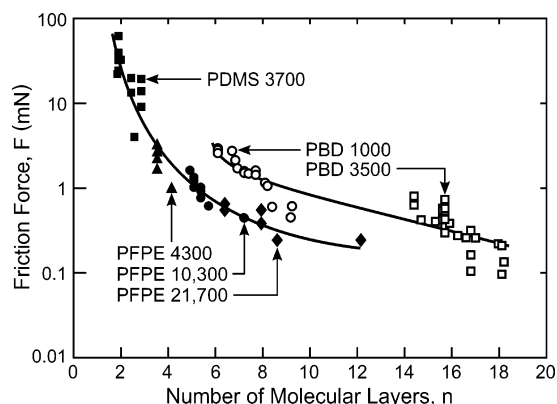


**Figure 7.** Friction force measured between mica surfaces separated by polymer melt thin films as a function of the molecular layering of the polymer melts. PDMS 3700 gives the highest friction and the lowest number of molecular layers between the surfaces whereas PBD 3500 gives the lowest friction and the highest number of molecular layers.

steeply when the number of molecular layers is less than 4. At low loads, low friction can be measured if the molecules do not get squeezed out from between the surfaces, regardless of chemistry and structure of the molecules. At separations beyond  $\sim 4R_g$ , the excess liquid between the surface layers appears to exhibit bulk viscosity.<sup>24</sup> Besides the loss of configurational entropy at small separations, adhesive bridging of the polymer chains may also occur as the film thickness decreases below some “critical thickness”, e.g., for  $D < R_g$ .<sup>20</sup> Bridging is expected to significantly increase the measured friction force.<sup>20,47</sup> This effect might be responsible for the unexpectedly high friction forces measured with the highly flexible PDMS 3700, where the film was unusually thin ( $D \sim R_g$ ), compared to the thicker films of PBD 1000 and PBD 3500 (cf. Figure 7). Further work needs to be done to establish whether the “critical thickness” should be defined or characterized in terms of the absolute thickness, the number of molecular layers, or the radius of gyration,  $R_g$ .

For the three different molecular masses of PFPE studied, the friction forces decrease as the bulk viscosity increases. However, between chemically distinct (homologously different) polymers, the friction coefficient is relatively independent of the bulk viscosity. For example, PFPE 4300 and PDMS 3700 have the same bulk viscosity, but the coefficients of friction differ by an order of magnitude.

The location of the shear, whether at the wall or within the lubricant film, depends on the interaction energies of the polymer chains with other polymer chains and also with the walls. Shear occurs where the yield stress or viscosity is smallest. Normally, Couette flow with no slip at the walls and a uniform shear gradient across the film is assumed. The friction force  $F$  or shear stress  $S$  between two parallel plates, separated by a Newtonian liquid, moving laterally relative to each other at velocity  $v$  is then given by

$$F = \eta A v / D$$

$$S = F/A = \eta v / D \quad (2)$$

where  $D$  is the surface separation,  $A$  is the area, and  $\eta$  is the viscosity. Using typical values measured in the experiments: for PBD 1000 of bulk viscosity  $\eta = 0.1$  Pa s (Table 1), a sliding velocity of  $v = 0.5 \mu\text{m/s}$ , and a film thickness of  $D = 3$  nm (Figure 5), we obtain a shear stress of  $S = 16$  Pa, which is 4 orders of magnitude smaller than the measured value of  $S = 0.27$  MPa (Figure 8). For all the polymers measured in this study, the “effective” viscosity was measured to be at least 2–4

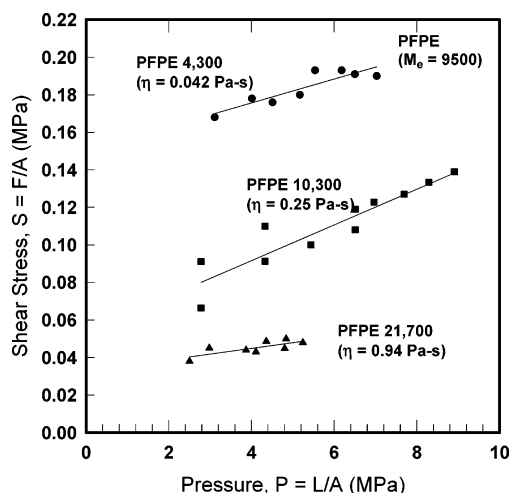


**Figure 8.** Measured shear stress as a function of the pressure between mica surfaces separated by thin polymer melt films. The solid lines are least-squares fit to the data. The shear stresses are measured to  $\pm 30\%$ .

orders of magnitude higher than the respective bulk viscosities. Confinement has previously been seen to increase the effective viscosity of simple molecules, and has been predicted for two-dimensional polymer films.<sup>18,25,48</sup> As already mentioned, the effective viscosity is proportionally higher for liquids with lower bulk viscosity.

Even allowing for the higher “effective” viscosities of fluids in molecularly thin films, eq 2 does not describe the observed dependence of  $F$  on  $A$ ,  $v$  and  $D$ . For constant contact area  $A$  and surface separation  $D$ , the friction force is predicted to be proportional to the sliding velocity  $v$ . In contrast, one finds the kinetic friction to be relatively insensitive to  $v$  for speeds between 0.5 and 3  $\mu\text{m/s}$ , both here and in previous studies,<sup>1,4,18</sup> in agreement with Coulomb’s law (but not eq 2 for Couette flow). In addition, in many cases one also observes a friction force that is roughly proportional to the load,  $L$  (cf. Figure 1), in agreement with Amontons’ Law. Equation 2 may therefore be rearranged for tribological (thin film shear, friction, and lubrication) forces as follows:

$$F = \eta_{\text{eff}} A v / D = \mu L \quad (3a)$$

or

$$S = \eta_{\text{eff}} v / D = \mu P \quad (3b)$$

where  $\mu$  is constant but where  $\eta_{\text{eff}}$  is no longer constant, and where  $D$  is determined by  $P$ . The results suggest two possibilities:

(1) In the tribological regime  $F \propto L$ ,  $\mu$  is roughly constant, and (at constant  $L$ ,  $P$ ,  $D$ ) independent of  $v$ . Thus,  $\eta_{\text{eff}} \propto 1/v$ , indicative of highly non-Newtonian, shear thinning behavior. As previously noted,<sup>11</sup> the high effective viscosities measured for such films are much higher than the enhanced viscosities of the bulk fluids subjected to similar hydrostatic pressures. Thus, some aspect of the confining surfaces, such as their molecular- or atomic-scale structure or “corrugations”, must play the key role in the “tribological” regime. The confining geometry (represented by the film thickness  $D$  but also includes the structures of the surfaces) is, of course, determined by the total load  $L$  or mean pressure  $P$ , but—as argued above— $L$  and  $P$  play an indirect role in determining the friction forces. This statement is not contradictory, since confinement within the bulk liquid is very different from confinement by two structured walls

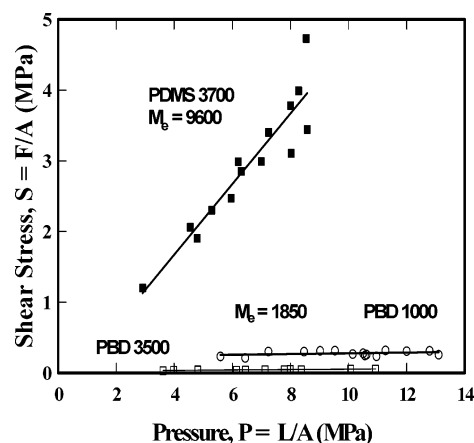


**Figure 9.** Measured shear stresses as a function of pressure between mica surfaces separated by thin films of PDMS 3700 (■), PBD 1000 (○), and PBD 3500 (□). The solid lines are a least-squares fit to the data. The shear stresses are measured to  $\pm 30\%$ .

under the same external (mean, isotropic) pressure  $P$ . Indeed, the distance  $D$  should, strictly, be written as  $D_{\text{eff}}$ , since for molecularly thin films it depends on the subnanoscale topography or structure of the confining surfaces.<sup>49</sup>

(2) The assumption of zero slip at the walls, inherent in eq 3, appears to break down in certain cases where there is full or partial slip at the walls rather than flow only within the film. Molecular-dynamics simulations also indicate that wall shear occurs for some films.<sup>40,50,51</sup> In these cases, a plug flow model with shear at the walls would be more appropriate.

To obtain more insight into the location of the shear plane, one may plot the shear stress  $S$  (friction/area) vs pressure  $P$  (load/area). According to eq 3b, even for a constant  $\mu$ ,  $S$  should increase with  $P$ . Yet for PBD we find that  $S$  is largely independent of  $P$  (Figure 9), and PFPE is also tending in that direction as its molecular mass increases (Figure 8). This supports the conclusion that wall shear is occurring. The results also give further support to the idea that it is the nature of the confinement, not the mean pressure, which influences the measured friction force.

On the other hand, the data for some of the other polymer melts, such as PDMS 3700, are consistent with a viscosity increase, so Couette-type flow could be occurring in such systems. The data for PFPE are intermediate, with a crossover from Couette flow to wall-slip occurring with increasing molecular mass (Figure 8). This crossover appears to depend on a number of factors, including the degree of entanglement in the polymer and the way the friction forces are measured: thus, the shear stress measured here for PFPE 4300 is an order of magnitude lower than previously reported values obtained using small-amplitude oscillatory shear measurements;<sup>17</sup> in those experiments, the shear amplitudes were less than 2  $\mu\text{m}$  and the contact areas were approximately  $5 \times 5 = 25 \mu\text{m}^2$ . In contrast, our measurements involved steady state (constant speed) sliding over much larger distances of 100  $\mu\text{m}$  and contact areas of approximately 3000  $\mu\text{m}^2$ . A number of studies have shown that the distance sheared (the shear amplitude or strain) is an important parameter that determines the steady-state friction forces, especially when complex molecules are involved that need to be sheared continuously over a certain large distance (often  $> 100 \mu\text{m}$  and/or over a larger distance than the diameter of the contact junction), but not time, before the film reaches its steady-state sliding configuration.<sup>12</sup> During this transitional “adaptation” stage, the friction force can fall by more than an order of magnitude (shear thinning effect), as was found for

squalane films.<sup>12</sup> Such effects do not seem to arise with small, symmetrical molecules where the steady-state friction sets in as soon as sliding commences. (In general, the friction coefficient is never a constant for any system of two surfaces, but depends on many experimental conditions in addition to the shearing distance.)

It is apparent that interchain entanglements play an important role in determining the shear properties of such systems. For nonentangled systems, internal shear in the film can occur, allowing for Couette-like flow.<sup>40</sup> Hence, PDMS 3700 might be expected to behave as other simple (non-polymeric) films where the shear occurs within the film. As the lubricant molecular mass increases, or if the chains are branched, the polymers become increasingly entangled and it becomes harder for the lubricants to shear *internally*. When the lubricant molecular mass exceeds the entanglement molecular mass,  $M_e$  (which may be different from the bulk value in a thin film), internal shear becomes extremely difficult and wall shear becomes an energetically favorable alternative.<sup>51</sup> Hence, a transition from internal shear within a film to wall slip may be expected to occur with increasing chain length and molecular "complexity" (asymmetry, branching, etc.). Measurements of confined films of the branched hydrocarbon squalane also indicate that wall shear can occur,<sup>52</sup> and Raviv et al.<sup>21</sup> found that in the shearing of adsorbed PEO layers in toluene the slip plane shifted from the polymer–polymer midplane to the polymer–substrate interface as the MW was increased from 37 000 g/mol to 112 000 g/mol. However, the idea of entanglements leading to wall-slip or "plug-flow" does not appear to be restricted to thin films but also to flow in bulk polymer melt systems.<sup>53,54</sup>

The subject of entanglements in *bulk* systems has been studied extensively.<sup>45,55</sup> However, for confined polymers, the theory of entanglements is less understood. The ratio of the polymer molecular mass to the entanglement molecular mass ( $M_w/M_e$ ) is 0.38, 0.65, and 2.27 for PDMS 3700, PBD 1000 and PBD 3500. PBD 3500 is entangled with a coefficient of friction of 0.006, and the coefficient of friction for PBD 7000 has been measured to be 0.008.<sup>19</sup> PFPE 21 700 ( $M_w/M_e = 2.28$ ) is also entangled in the bulk, with a measured friction coefficient of 0.008. Hence, it appears that a lower limit of  $\sim 0.006$  in the friction coefficient is reached when the polymers are entangled. Shear at the wall is favored in these entangled systems giving rise to the low friction coefficient and pressure-independent shear stress.

Enhanced entanglements in thin films also gives rise to reduced mobility of the polymer chains and hence longer relaxation times.<sup>18</sup> This has already been observed for shorter hydrocarbons such as hexadecane and 2-methyloctadecane, where the relaxation time is orders of magnitude longer than in unconfined systems.<sup>11,34,56</sup> The confined fluids tend to behave more as glassy materials than as liquids. The bulk glass transition temperature is  $-80^\circ\text{C}$  for PBD, which means there is a dramatic change in the mobility of these confined thin films. Frequency-dependent shear response measurements as well as reflectivity measurements also show enhanced entanglements of polymer melts when the film thickness is less than  $3-6R_g$ .<sup>18,57</sup>

For wall slip to occur in entangled polymer melts, the monomer chemistry must also be important. Materials with polar end groups might interact more strongly with the solid surface and more readily resist wall slip. For example, the addition of hydroxy end groups to PFPE improves its resistance to being squeezed out from between sliding silicon surfaces.<sup>29</sup> On the macroscopic scale, all the melts were found to wet the mica surfaces with an advancing contact angle of less than  $10^\circ$ ,

indicating a favorable interaction of all the melts with the mica surfaces.

Recently, the friction of polymer melt films was measured with an atomic force microscope (AFM) and the results compared to measurements with the SFA.<sup>58</sup> In the AFM measurements using a sharp probe tip, the coefficient of friction between two different polymers gave similar friction. For the mobile films in the AFM experiments, the high pressures of the sharp AFM tip likely squeezed the polymers out from the contact. The low friction measured with the SFA was measured at relatively large contact areas and lower pressures where a constant film thickness was maintained. Sivebaek et al.<sup>35</sup> simulated small *n*-alkane molecules ( $\text{C}_3\text{H}_8$  to  $\text{C}_{14}\text{H}_{30}$ ) showing that the longer chained alkanes require higher pressures to be squeezed out from between two surfaces. Since the polymer molecules used in our study are much longer and have a more varied structure than simple *n*-alkanes, it is difficult to make a direct comparison. However, previous results with small or short-chained hydrocarbon molecules<sup>8,10,59</sup> have shown that they can be squeezed out at sufficiently high loads, while all the (higher molecular mass) polymer melt films studied here cannot. Our results further show that the higher molecular mass films are thicker and can give very low friction coefficients, as low as 0.006, but that this is probably due to wall slip (without squeeze out). Thus, wall-slip may give the lowest friction in some systems.

## Conclusions

The friction properties of the confined polymer melts poly-(dimethylsiloxane), polybutadiene, and perfluoropolyether were measured. The friction forces were proportional to the load and no intermittent or stick–slip sliding was observed. PDMS 3700 gave the highest coefficient of friction ( $\mu = 0.48$ ), a value that is similar to those of short linear hydrocarbon chains. Polybutadiene and perfluoropolyether gave very low friction coefficients, between 0.023 and 0.006.

In general, as we go from low molecular mass alkanes to high molecular mass polymer melts, the friction coefficients decrease with increasing molecular mass and bulk viscosity, and the friction for (the usually higher molecular mass) entangled systems is lower than for nonentangled systems as film-slip transforms into wall-slip. Wall slip was inferred when the shear stress did not vary with pressure, film thickness, or velocity. However, there appears to be a lower limit for the value of the friction coefficient, of about 0.005, once the polymers are fully entangled in the bulk, presumably because the interfacial shear stress at wall no longer depends on the molecular length.

Some shear ordering of the molecules into layers occurs as the molecules are confined. Lateral motion enabled the PDMS and PFPE to be more easily ordered and removed from the contact zone, whereas the entangled PBD melt is more difficult to remove. At high loads, the more flexible molecules, PDMS and PFPE, are able to keep the surfaces separated by  $\sim 1R_g$ , whereas the more rigid PBD polymer has a minimum surface separation of  $\sim 5R_g$ . Thus, PBD appears to have good load bearing capability due to the high entanglements between the chains and a stiff backbone, in addition to exhibiting low friction.

**Acknowledgment.** The authors would like to thank Mark Robbins, Jack Douglas, Uzi Landman, and Marina Ruths for helpful suggestions. This work was supported by the Department of Energy under Grant DE-FG02-87ER45331.



## References and Notes

- (1) Bowden, F. P.; Tabor, D. *The Friction and Lubrication of Solids*; Clarendon Press: Oxford, U.K., 1986.
- (2) Tabor, D. *Macroscopic Aspects of Adhesion and Lubrication*; Elsevier Scientific Publishing Co.: New York, 1982; p 651.
- (3) Appeldoorn, J. K. *Boundary Lubrication, An Appraisal of World Literature*; American Society of Mechanical Engineers: New York, 1969; p 133.
- (4) Ruths, M.; Berman, A.; Israelachvili, J. *Nanotribology and Nanomechanics: An Introduction*; Springer-Verlag: Berlin, 2005; p 389.
- (5) Dowson, D. *History of Tribology*; Longman: New York, 1979.
- (6) Fein, R. S. *CRC Handbook of Lubrication, Theory and Practice of Tribology, II, Theory and Design*; CRC Press: Boca Raton, FL, 1984.
- (7) *Handbook of Micro/Nanotribology*; CRC Press: Boca Raton, FL, 1995.
- (8) Israelachvili, J. N.; McGuiggan, P. M.; Homola, A. M. *Science* **1988**, 240 (4849), 189.
- (9) Homola, A. M.; Israelachvili, J. N.; Gee, M. L.; McGuiggan, P. M. *J. Tribol.—Trans. ASME* **1989**, 111, 675.
- (10) Gee, M. L.; McGuiggan, P. M.; Israelachvili, J. N.; Homola, A. M. *J. Chem. Phys.* **1990**, 93, 1895.
- (11) Drummond, C.; Israelachvili, J. *Phys. Rev. E* **2001**, 6304 (4).
- (12) Drummond, C.; Israelachvili, J. *Macromolecules* **2000**, 33, 4910.
- (13) Gourdon, D.; Israelachvili, J. N. *Phys. Rev. E* **2003**, 68 (2).
- (14) Klein, J.; Kumacheva, E.; Mahalu, D.; Perahia, D.; Fetters, L. J. *Nature* **1994**, 37 (6491), 634.
- (15) Yamada, S.; Nakamura, G.; Amiya, T. *Langmuir* **2001**, 17, 1693.
- (16) Yamada, S. *Langmuir* **2003**, 19, 7399.
- (17) Ruths, M.; Granick, S. *Tribol. Lett.* **1999**, 7 (4), 161.
- (18) Hu, H. W.; Granick, S. *Science* **1992**, 258 (5086), 1339.
- (19) Luengo, G.; Schmitt, F. J.; Hill, R.; Israelachvili, J. *Macromolecules* **1997**, 30, 2482.
- (20) Hirz, S.; Subbotin, A.; Frank, C.; Hadziioannou, G. *Macromolecules* **1996**, 29, 3970.
- (21) Raviv, U.; Tadmor, R.; Klein, J. *J. Phys. Chem. B* **2001**, 105, 8125.
- (22) Horn, R. G.; Israelachvili, J. N.; Pribac, F. J. *Colloid Interface Sci.* **1987**, 115, 480.
- (23) Horn, R. G.; Israelachvili, J. N. *Macromolecules* **1988**, 21, 2836.
- (24) Israelachvili, J. N.; Kott, S. J. *J. Chem. Phys.* **1988**, 88, 7162.
- (25) Israelachvili, J. N.; McGuiggan, P. M.; Homola, A. M. *Science* **1988**, 240 (4849), 189.
- (26) Colby, R. H.; Fetters, L. J.; Graessley, W. W. *Macromolecules* **1987**, 20, 2226.
- (27) Rubinstein, M.; Colby, R. H. *Polymer Physics*; Oxford University Press: New York, 2003.
- (28) Fetters, L. J.; Lohse, D. J.; Richter, D.; Witten, T. A.; Zirkel, A. *Macromolecules* **1994**, 27, 4639.
- (29) Mate, C. M. *Phys. Rev. Lett.* **1992**, 68, 3323.
- (30) Marchionni, G.; Ajroldi, G.; Pezzin, G. *Comprehensive Polymer Science*; Pergamon Press: New York, 1996; p 347.
- (31) Cantow, M. J. R.; Larrabee, R. B.; Barrall, E. M.; Butner, R. S.; Cotts, P.; Levy, F.; Ting, T. Y. *Makromol. Chem.—Macromol. Chem. Phys.* **1986**, 187, 2475.
- (32) Cotts, P. M. *Macromolecules* **1994**, 27, 6487.
- (33) van Krevelen, D. W. *Properties of Polymers: Correlations With Chemical Structure*; Elsevier: Amsterdam, 1972.
- (34) Gee, M. L.; McGuiggan, P. M.; Israelachvili, J. N.; Homola, A. M. *J. Chem. Phys.* **1990**, 93, 1895.
- (35) Sivebaek, I. M.; Samoilov, V. N. P. B. N. J. *J. Chem. Phys.* **2003**, 119, 2314.
- (36) Horn, R. G.; Hirz, S. J.; Hadziioannou, G.; Frank, C. W.; Catala, J. M. *J. Chem. Phys.* **1989**, 90, 6767.
- (37) Montfort, J. P.; Hadziioannou, G. *J. Chem. Phys.* **1988**, 88, 7187.
- (38) Yoshizawa, H.; Israelachvili, J. J. *Phys. Chem.* **1993**, 97, 11300.
- (39) Jabbarzadeh, A.; Atkinson, J. D.; Tanner, R. I. *J. Chem. Phys.* **1999**, 110, 2612.
- (40) Thompson, P. A.; Robbins, M. O. *Science* **1990**, 250 (4982), 792.
- (41) Thompson, P. A.; Grest, G. S.; Robbins, M. O. *Phys. Rev. Lett.* **1992**, 68, 3448.
- (42) Israelachvili, J.; McGuiggan, P.; Gee, M.; Homola, A.; Robbins, M.; Thompson, P. J. *Phys.—Condens. Matter* **1990**, 2SA89.
- (43) Gao, J. P.; Luedtke, W. D.; Landman, U. *J. Chem. Phys.* **1997**, 106, 4309.
- (44) Dolan, A. K.; Edwards, S. F. *Proc. R. Soc. London, Ser. A—Math. Phys. Eng. Sci.* **1974**, 337 (1611), 509.
- (45) Doi, M.; Edwards, S. F. *The Theory of Polymer Dynamics*; Oxford University Press: Oxford, U.K., 1988.
- (46) Casassa, E. F. *J. Polym. Sci. Part B—Polym. Lett.* **1967**, 5 (9PB), 773.
- (47) Kampf, N.; Raviv, U.; Klein, J. *Macromolecules* **2004**, 37, 1134.
- (48) Douglas, J. F.; Hubbard, J. B. *Macromolecules* **1991**, 24, 3163.
- (49) Israelachvili, J.; Maeda, N.; Rosenberg, K. J.; Akbulut, M. *J. Mater. Res.* **2005**, 20, 1952.
- (50) Thompson, P. A.; Grest, G. S.; Robbins, M. O. *Phys. Rev. Lett.* **1992**, 68, 3448.
- (51) Thompson, P. A.; Robbins, M. O.; Grest, G. S. *Isr. J. Chem.* **1995**, 35, 93.
- (52) Reiter, G.; Demirel, A. L.; Peanasky, J.; Cai, L. L.; Granick, S. *J. Chem. Phys.* **1994**, 101, 2606.
- (53) Mhetar, V.; Archer, L. A. *Macromolecules* **1998**, 31, 6639.
- (54) Robert, L.; Demay, Y.; Vergnes, B. *Rheol. Acta* **2004**, 43, 89.
- (55) Ferry, J. D. *Viscoelastic Properties of Polymers*; New York, 1980.
- (56) Yoshizawa, H.; Israelachvili, J. J. *Phys. Chem.* **1993**, 97, 11300.
- (57) Wallace, W. E.; vanZanten, J. H.; Wu, W. L. *Phys. Rev. E* **1995**, 52, R3329.
- (58) McGuiggan, P. M.; Zhang, J.; Hsu, S. M. *Tribol. Lett.* **2001**, 10 (4), 217.
- (59) Homola, A. M.; Israelachvili, J. N.; McGuiggan, P. M.; Gee, M. L. *Wear* **1990**, 136 (1), 65.

MA061750H